OPEN ACCESS
IOP PUBLISHING
SCIENCE AND TECHNOLOGY OF ADVANCED MATERIALS
Sci. Technol. Adv. Mater. **14** (2013) 035002 (8pp)
doi:10.1088/1468-6996/14/3/035002

Tissue-engineered endothelial cell layers on surface-modified Ti for inhibiting *in vitro* platelet adhesion

Xiupeng Wang[1], Fupo He[2,3], Xia Li[1], Atsuo Ito[1], Yu Sogo[1], Osamu Maruyama[2], Ryo Kosaka[2] and Jiandong Ye[3,4]

[1] Human Technology Research Institute, National Institute of Advanced Industrial Science and Technology (AIST), Central 6, 1-1-1 Higashi, Tsukuba, Ibaraki 305-8566, Japan
[2] Human Technology Research Institute, National Institute of Advanced Industrial Science and Technology (AIST), Namiki1-2-1, Tsukuba, Ibaraki 305-8564, Japan
[3] School of Materials Science and Engineering, South China University of Technology, Guangzhou 510641, People's Republic of China
[4] National Engineering Research Center for Tissue Restoration and Reconstruction, Guangzhou 510006, People's Republic of China

E-mail: xp-wang@aist.go.jp

Received 13 December 2012
Accepted for publication 15 April 2013
Published 15 May 2013
Online at stacks.iop.org/STAM/14/035002

Abstract
A tissue-engineered endothelial layer was prepared by culturing endothelial cells on a fibroblast growth factor-2 (FGF-2)–L-ascorbic acid phosphate magnesium salt *n*-hydrate (AsMg)–apatite (Ap) coated titanium plate. The FGF-2–AsMg–Ap coated Ti plate was prepared by immersing a Ti plate in supersaturated calcium phosphate solutions supplemented with FGF-2 and AsMg. The FGF-2–AsMg–Ap layer on the Ti plate accelerated proliferation of human umbilical vein endothelial cells (HUVECs), and showed slightly higher, but not statistically significant, nitric oxide release from HUVECs than on as-prepared Ti. The endothelial layer maintained proper function of the endothelial cells and markedly inhibited *in vitro* platelet adhesion. The tissue-engineered endothelial layer formed on the FGF-2–AsMg–Ap layer is promising for ameliorating platelet activation and thrombus formation on cardiovascular implants.

Keywords: endothelial cell, platelet adhesion, fibroblast growth factor-2, ascorbate, apatite

1. Introduction

Blood-contacting implants benefit millions of patients with cardiovascular disease; however, thrombus and embolus are often formed on the blood-contacting surfaces, causing significant morbidity and mortality [1–3]. Usually, anti-platelet agents or anticoagulants are used to reduce the risk of these adverse events, which predispose the patients to bleeding complications [4, 5]. Anti-thrombogenic or anti-inflammatory drug-coated vascular stents have recently proven to be problematic in healing atherosclerotic blood vessels [6, 7].

A tissue-engineered endothelial cell layer on the blood-contacting surface would provide the blood-contacting implants with excellent anti-thrombogenic and anti-inflammatory effects [1], as the endothelium is the physiological and most hemocompatible blood-contacting surface. A tissue-engineered endothelial cell layer that represents an inherent non-thrombogenic potential on the blood-contacting surface not only provides a non-adhesive surface for platelets and leukocytes but also produces a variety of important biomolecules such as endothelin, prostaglandins and nitric oxide (NO) [8–11].

The major limitation to forming a tissue-engineered endothelium surface has been the shortage of an extracellular matrix suitable for endothelialization. Biomolecules are widely used for promoting endothelialization. For example, fibroblast growth factor-2 (FGF-2) is a heparin binding growth factor that stimulates the proliferation of a wide variety of cells, including endothelial cells [12–14]. Ascorbate, for example L-ascorbic acid phosphate magnesium salt *n*-hydrate (AsMg), has been used to prevent endothelial dysfunction [15, 16]. However, the biomolecules are highly susceptible to physiological diffusion and degradation processes, leading to a short half-life [17–19]. Apatite is a promising matrix for immobilizing biomolecules with increasing biomolecule stability and promoting persistent signaling [20–27]. Besides, apatite, as the main inorganic component of human hard tissues, has good biocompatibility and has been reported to show good thromboresistance [28].

We hypothesize that the FGF-2–AsMg–apatite (FAsAp) layer is a promising extracellular matrix for endothelialization, which can accelerate endothelial cell proliferation and maintain proper function of the endothelial cells. In this study, a FAsAp layer was formed on the titanium plate followed by formation of a layer of tissue-engineered human umbilical vein endothelial cells (HUVECs) on the FAsAp layer. *In vitro* platelet adhesion to the tissue-engineered HUVEC layer was also tested.

2. Materials and methods

2.1. Preparation of Ti plates

Commercially available Ti sheets (1 × 100 × 300 mm, Nilaco Corporation, Japan) were cut into square plates (1 × 11 × 11 mm) using a silicon carbide blade. The Ti plates were ultrasonically washed with acetone for 30 min and then dried at room temperature. Then, the Ti plates were heated from room temperature to 300 °C at a heating rate of 1 °C h^{-1}, and annealed at 300 °C for 2 h.

2.2. Preparation of solutions

A calcium-containing solution (4.5 mM Ca^{2+}, ×2.0 Ringer's) was obtained by mixing Ringer's solution (Otsuka, 2.25 mM Ca^{2+}) and Conclyte®-Ca (Otsuka, 500 mM Ca^{2+}). An FGF-2 solution with a concentration of 100 μg ml^{-1} was prepared by dissolving FGF-2 (Fiblast®, Kaken Pharmaceutical Co., Ltd, Japan) in ×2.0 Ringer's followed by filter sterilization using a membrane with a pore size of 0.22 μm (×2.0 Ringer's–FGF-2). The FGF-2 reagent is a pharmaceutical human-recombinant FGF-2 containing undisclosed amounts of sucrose, ethylene diamine tetraacetic acid (EDTA) and a pH adjustment agent. An AsMg solution with a concentration of 2500 μg ml^{-1} was prepared by dissolving AsMg (Wako Pure Chemical Industry Ltd, Japan) in ×2.0 Ringer's followed by filter sterilization using a membrane with a pore size of 0.22 μm (×2.0 Ringer's–AsMg). A phosphate-containing solution (20 mM PO_4^{3-}, ×2.0 Klinisalz® B) was obtained by mixing Klinisalz® B (I'rom Pharmaceutical Co., Ltd, Japan, 10 mM PO_4^{3-}) and Conclyte® solution-PK (Otsuka, 500 mM PO_4^{3-}). An alkalinizer, Bifil® (Ajinomoto Pharma, Japan), was used as received without changing its original concentration. Supersaturated calcium phosphate solutions were prepared by mixing ×2.0 Ringer's, ×2.0 Ringer's–FGF-2, ×2.0 Ringer's–AsMg, ×2.0 Klinisalz® B and alkalinizer at the mixing ratio shown in table 1. The chemical compositions of the supersaturated calcium phosphate solutions are shown in table 2. All the solutions used in this study were infusion fluids clinically available in Japan. The merits of using clinically approved pharmaceutical formulations are that they are sterile and endotoxin free, and have a low regulatory barrier for clinical applications [20–25, 29–31].

Table 1. Supersaturated calcium phosphate solutions.

Total volume (ml)	×2.0 Ringer's (ml)	×2.0 Ringer's–FGF-2 (ml)	×2.0 Ringer's–AsMg (ml)	×2.0 Klinisalz® B (ml)	Alkalinizer (ml)
5	3.69–4.09	0–0.2	0–0.2	0.46	0.45

Table 2. Chemical components of supersaturated calcium phosphate solutions

Component	Ap	FAp	AsAp	FAsAp
Na^+ (mM)	138.75	138.75	138.75	138.75
K^+ (mM)	7.37	7.37	7.37	7.37
Ca^{2+} (mM)	3.68	3.68	3.68	3.68
Mg^{2+} (mM)	0.22	0.22	0.22	0.22
Cl^- (mM)	134.27	134.27	134.27	134.27
$H_2PO_4^-$ (mM)	0.90	0.90	0.90	0.90
HPO_4^{2-} (mM)	0.94	0.94	0.94	0.94
HCO_3^- (mM)	15.09	15.09	15.09	15.09
CH_3COO^- (mM)	1.80	1.80	1.80	1.80
FGF-2 (μg ml^{-1})	0	4	0	4
AsMg (μg m1^{-1})	0	0	100	100

2.3. Formation of apatite (Ap), FGF-2–apatite (FAp), AsMg–apatite (AsAp) and FGF-2–AsMg–apatite (FAsAp) layers on Ti plates

The Ti plates were sterilized at 160 °C for 3 h in a dry sterilizer (model SG600, Yamato Scientific, Co., Ltd). After being cooled to room temperature, each Ti plate was aseptically immersed in 5 ml of the supersaturated calcium phosphate solutions (table 2) at 37 °C for 48 h to obtain the coatings of Ap, FAp, AsAp and FAsAp. After the immersion, the coatings were mildly washed by immersing in 2 ml of ultrapure water for 3 min.

2.4. Surface characterization of Ti plates

Before the surface analysis, the washed Ti plates were freeze-dried. The surface morphology of the Ti plates was analyzed by field emission scanning electron microscopy (FE-SEM, S-4800, Hitachi, Japan) at an accelerating voltage of 10 kV after being coated with platinum. The coatings removed from the Ti surfaces were observed with transmission electron microscopy (TEM). When the Ti

plates were found to be covered by precipitated layers, the precipitated layers were scraped off from the Ti plates and analyzed by x-ray diffraction (XRD) employing Cu Kα x-rays at 40 kV and 300 mA using a powder x-ray diffractometer (model RINT 2400; Rigaku, Japan) and a silicon-zero-background plate. The 2θ scanning range and speed were 20–80° and 1° min^{-1}, respectively. Fourier transform infrared spectra (FTIR) were recorded using an FTIR-350 spectrometer (Jasco Corporation, Japan) by the KBr pellet method.

2.5. Measurements of amounts of calcium, phosphorus, FGF-2 and AsMg in the Ap, FAp, AsAp and FAsAp layers

The Ti plates with Ap, FAp, AsAp and FAsAp layers were immersed in 5 ml of a citric acid buffer (10 mM, pH 5.43) at 25 °C overnight to extract the calcium, phosphorus, AsMg and FGF-2 completely by dissolving the layers. The complete dissolution of the layers was confirmed by scanning electron microscopy (FE-SEM). The amounts of precipitated calcium and phosphorus were measured using an inductively coupled plasma atomic emission spectrometer (ICP: SPS7800, Seiko Instruments, Inc.). The amount of precipitated FGF-2 was measured by the Bradford method using a Bio-Rad protein assay dye reagent concentrate (Bio-Rad Laboratories, Inc., Japan) in accordance with the manufacturer's instructions. The amounts of precipitated AsMg were determined by measuring the UV absorption band intensity of AsMg at 235 nm using a UV–visible spectrophotometer (V-550, Jasco, Japan).

2.6. In vitro HUVEC proliferation on Ap, FAp, AsAp and FAsAp coated Ti plates

HUVECs with a concentration of 5×10^5 cells ml^{-1} were placed on the Ap, FAp, AsAp and FAsAp coated Ti plates and cultured in a humidified atmosphere of 5% CO_2 at 37 °C for 3 days. The culture medium used was endothelial basal medium-2 EBM®-2 supplemented with 2% fetal bovine serum and growth factors (Lonza Walkersville, Inc., USA) according to the manufacturer's protocols. The proliferation level of HUVECs was determined by the WST-8 method using a CCK-8 kit (Dojindo Laboratories, Japan) in accordance with the manufacturer's instructions.

2.7. Nitric oxide (NO) release from HUVECs on as-prepared Ti, Ap and FAsAp coated Ti plates

NO produced by the vascular endothelium is an important biological messenger that inhibits leukocyte and platelet adhesion and aggregation. NO deficiency increases thrombosis due to platelet aggregation and adhesion to the vascular endothelium.

HUVECs were seeded and cultured under the same conditions as described in section 2.6. NO release from HUVECs on as-prepared Ti, Ap and FAsAp coated Ti plates after 3 days of culture was tested using a Total NO/Nitrite/Nitrate kit (R&D systems) in accordance with the manufacturer's instructions.

2.8. Platelet adhesion to Ti, Ap and FAsAp+HUVEC coated Ti plates

The tissue-engineered Ti plates were prepared by culturing 5×10^5 cells ml^{-1} of HUVECs on the FAsAp coated Ti plates as described in section 2.6. After 3 days of culture, the culture medium was replaced by 1 ml of 2 μM CellTracker™ Green (Invitrogen, Ltd, UK) in a humidified atmosphere of 5% CO_2 at 37 °C for 30 min. Then, the tissue-engineered (FAsAp+HUVEC coated) Ti plates were washed with phosphate-buffered saline (PBS(-))2 times.

Fresh rat blood (2 m1) was drawn and mixed with 150 μl of 0.077 M EDTA·2Na. Plasma was obtained by centrifuging the rat blood solution at 2000 rpm for 10 min. Platelet-rich plasma was obtained by centrifuging the plasma at 4000 rpm for 10 min. Platelet-rich plasma was suspended in 2 ml of 2 μM CellTracker™ Orange (Invitrogen, Ltd, UK) in a humidified atmosphere of 5% CO_2 at 37 °C for 30 min. Then, the platelet-rich plasma was washed twice using 10 ml PBS(-) and centrifuged at 4000 rpm for 10 min to discard the residual dye reagent and suspended at a concentration of 1×10^4 platelets ml^{-1} in PBS(-).

Ti, Ap and FAsAp + HUVEC coated Ti plates were immersed in 1 ml of 1×10^4 platelets ml^{-1} and incubated in a humidified atmosphere of 5% CO_2 at 37 °C for 2 h. After washing with PBS(-), the HUVECs and platelets adhering to the Ti, Ap and FAsAp + HUVEC layers were observed using a fluorescent staining and fluorescence microscope (BX51, Olympus, Japan). The amounts of platelet that adhered to the Ti, Ap and FAsAp + HUVEC layers were calculated using Image-Pro® Plus software (Media Cybernetics, Inc., version 7.0). For each sample, eight–ten samples were selected for quantitative analysis.

3. Results

FE-SEM images of the bare Ti plate, and Ap, FAp, AsAp and FAsAp coated Ti plates are shown in figure 1. A continuous and homogeneous layer consisting of flake-shaped fine particles was formed on the Ap or FAp coated Ti plates (figure 1, Ap, FAp). On the AsAp or FAsAp coated Ti plates, not flake-shaped but round-shaped particles were observed (figure 1, AsAp, FAsAp). The coatings removed on the Ti plates were observed further using TEM (figure 2). Ap or FAp showed micro-sized particles, while AsAp or FAsAp showed nano-sized particles. AsMg obviously inhibited the crystal growth of the precipitates.

The XRD patterns of the bare Ti and the surface layers scraped from the Ti plates are shown in figure 3. All the surface layers consist of low-crystalline apatite, as proved by the broad peaks at 25.8 and 31.8° (ICDD no. 09-432).

The FTIR spectra of the surface layers scraped from the Ti plates are shown in figure 4. Carbonate bands appeared at 1450, 1420 and 872 cm^{-1}. PO_4^{3-} bands appeared at 1090–1030, 603 and 565 cm^{-1}. Bands for adsorbed H_2O appeared at 1600–1670 and 3000–3600 cm^{-1}.

Figure 5 shows the amounts of calcium and phosphorus precipitated on the Ti plates. FGF-2 and AsMg alone or

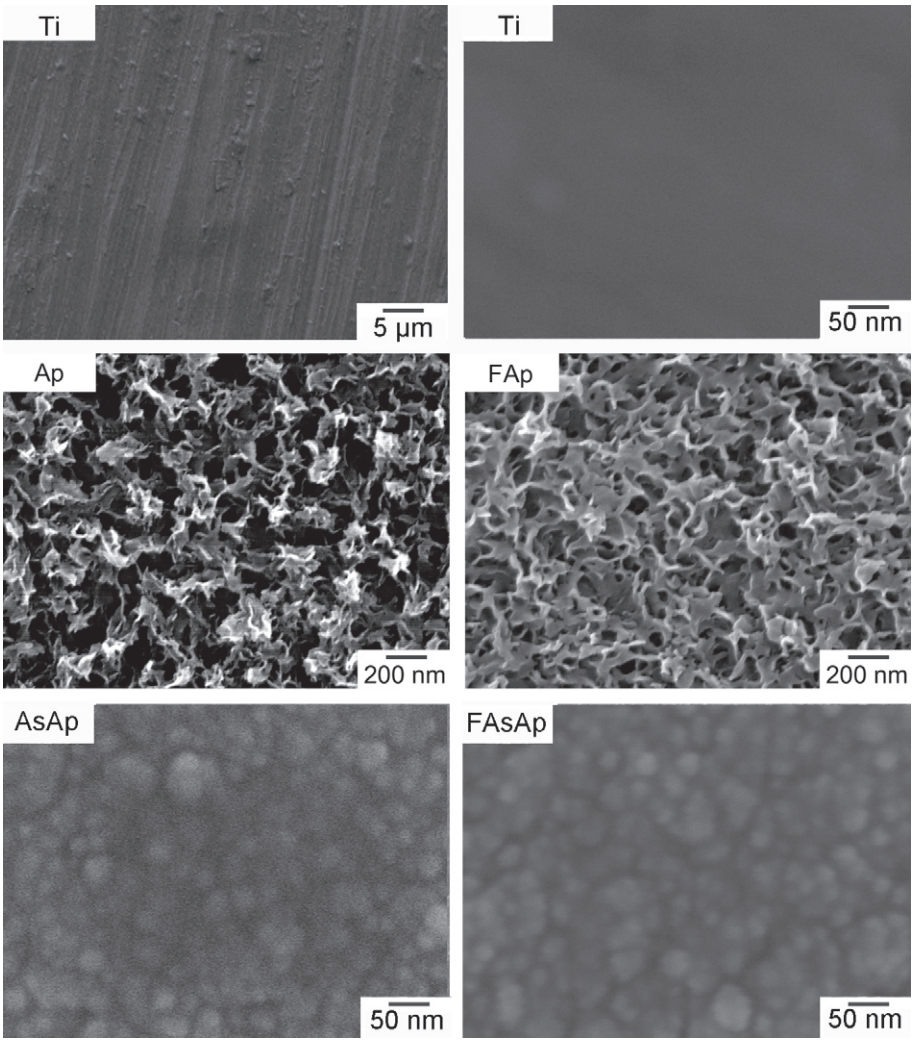

Figure 1. FE-SEM images of the bare Ti plate and Ap, FAp, AsAp and FAsAp coatings on Ti plates.

in combination greatly inhibited the precipitation of apatite. The amounts of calcium precipitated were 93 ± 21, 71 ± 23, 37 ± 6 and $28 \pm 4\,\mu$g per plate for Ap, FAp, AsAp and FAsAp, respectively. The amounts of phosphorus precipitated were 55 ± 13, 44 ± 12, 28 ± 4 and $21 \pm 3\,\mu$g per plate for Ap, FAp, AsAp and FAsAp, respectively.

Figure 6 shows the amounts of precipitated FGF-2 and AsMg on Ti plates. AsMg significantly inhibited the precipitation of FGF-2. The amounts of FGF-2 immobilized on FAp and FAsAp layers were 12 ± 1 and $10 \pm 1\,\mu$g per plate, respectively. FGF-2 significantly inhibited the precipitation of AsMg. The amounts of AsMg immobilized on AsAp and FAsAp layers were 109 ± 76 and $41 \pm 2\,\mu$g per plate, respectively.

HUVEC proliferation on Ti, Ap, FAp, AsAp and FAsAp coated Ti plates after 3 days of culture is shown in figure 7. FGF-2 or AsMg promoted the proliferation of HUVECs. The number of HUVECs on FAp and AsAp was higher than those on Ti. The combination of FGF-2 and AsMg showed greater proliferation of HUVECs than those with FGF-2 or AsMg. However, the number of HUVECs on FAsAp coated Ti plates was only slightly higher than those on FAp coated Ti plates. The number of HUVECs on FAsAp coated Ti plates was significantly higher than those on Ti and AsMg coated Ti plates. Therefore, FAsAp coated Ti plates were selected as the matrix for growing a tissue-engineered HUVEC layer (FAsAp + HUVEC).

Nitric oxide release from tissue-engineered HUVECs on as-prepared Ti, Ap and FAsAp coated Ti plates after 3 days of culture is shown in figure 8. HUVECs on FAsAp coated Ti showed a slightly higher NO content than on Ap coated and as-prepared Ti.

Fluorescence microscopy images of platelets adhered to Ti, Ap and tissue-engineered HUVEC coated Ti are shown in figure 9. A large number of platelets were observed on Ti and Ap coated Ti plates. Brick-like HUVEC cells fully covered the surface of FAsAp coated Ti plates. Only a small number of platelets were observed on the tissue-engineered HUVEC coated Ti plates. Quantitative analysis of the number of platelets according to the fluorescence microscopy images is presented in figure 10. Both Ap and tissue-engineered HUVEC coated Ti plates significantly restricted the platelet adhesion. Tissue-engineered HUVEC coated Ti plates showed a significantly decreased number of adhered platelets than

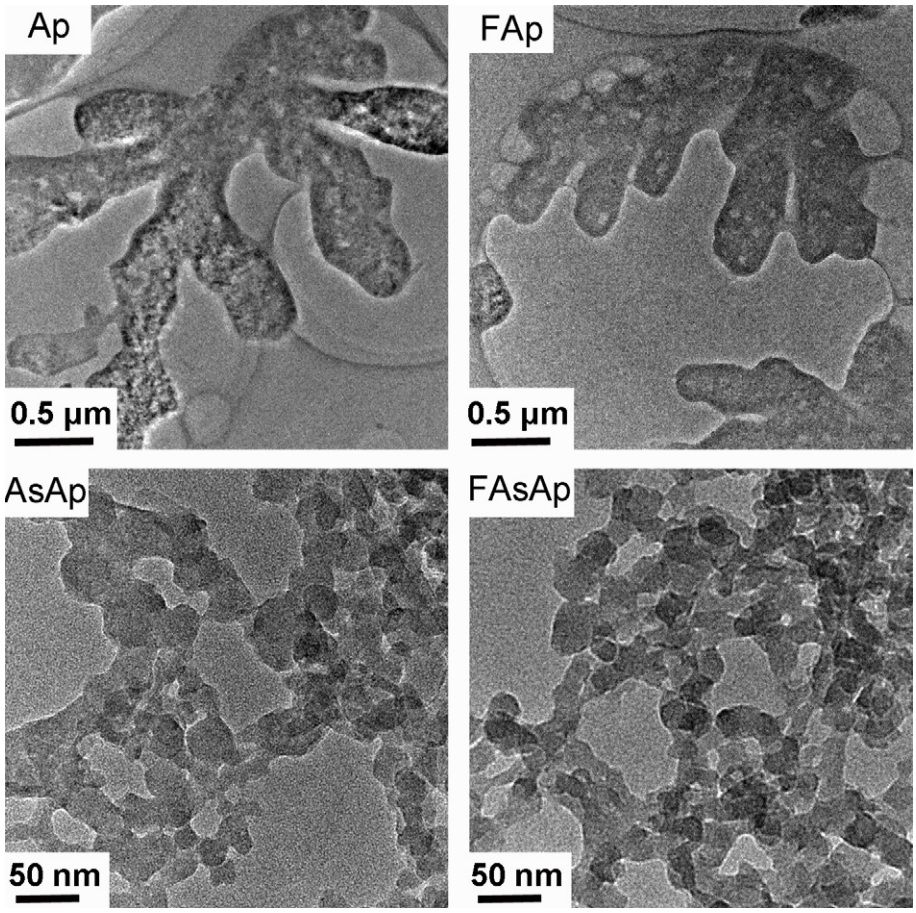

Figure 2. TEM images of Ap, FAp, AsAp and FAsAp coatings on Ti plates.

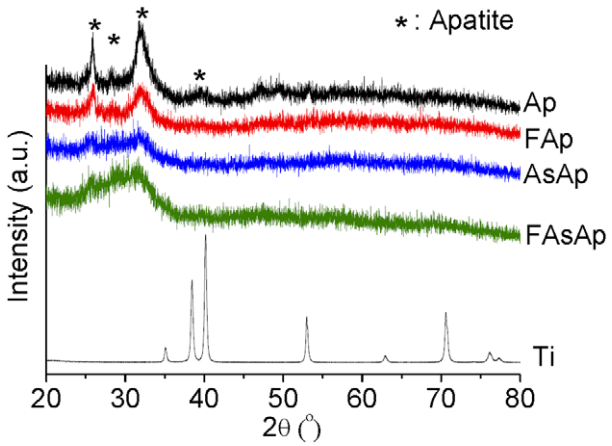

Figure 3. XRD patterns of Ti, Ap, FAp, AsAp and FAsAp coatings on Ti plates.

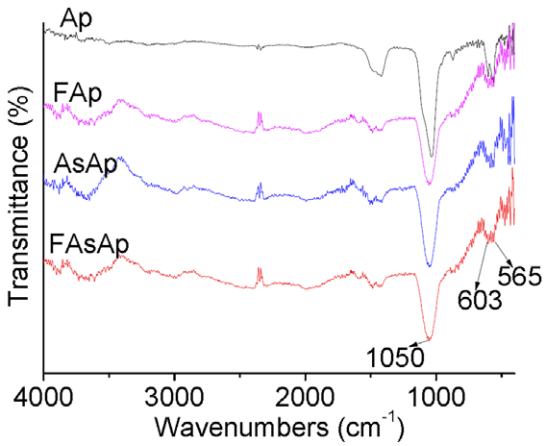

Figure 4. FTIR spectra of Ap, FAp, AsAp and FAsAp coatings on Ti plates. The spectra are offset vertically for clarity.

those on Ap coated Ti plates. The number of platelets adhered to Ti, Ap and tissue-engineered HUVEC coated Ti were 54 ± 13, 33 ± 3 and 15 ± 5 platelets mm^{-2}, respectively.

4. Discussion

Rapid growth as well as maintenance of proper function of endothelial cells is potentially beneficial in inhibiting platelet adhesion and thrombosis formation. The FGF-2–AsMg–Ap layer on Ti plates accelerated proliferation and maintained proper function of endothelial cells. The tissue-engineered endothelial layer markedly inhibited platelet adhesion *in vitro*.

The FGF-2–AsMg–Ap layer provided a suitable extracellular matrix for rapid endothelialization. In our previous study, the FGF-2–AsMg–Ap layer on Ti rods markedly enhanced the proliferation of fibroblastic

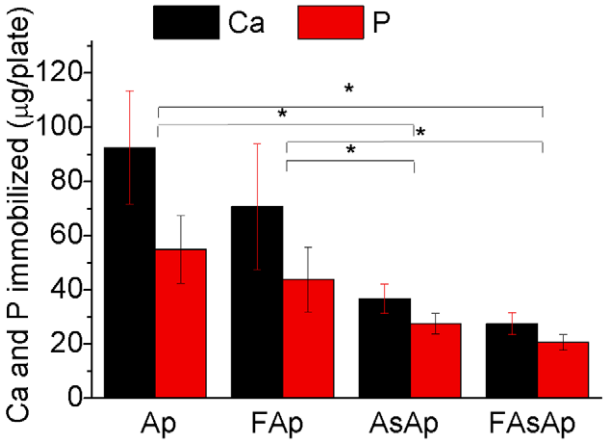

Figure 5. Amount of Ca and P immobilized on Ti plates.

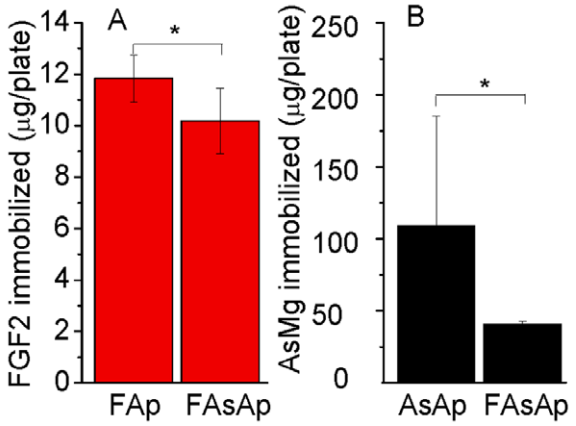

Figure 6. Amount of FGF-2 and AsMg immobilized on Ti plates.

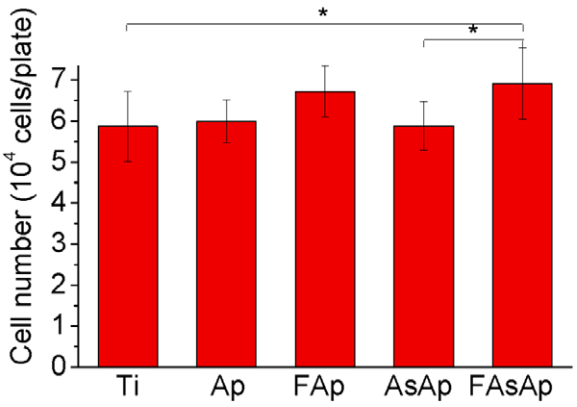

Figure 7. HUVEC proliferation on Ap, FAp, AsAp and FAsAp coated Ti plates after 3 days of culture.

NIH3T3 cells and osteoblastic MC3T3-E1 cells, but inhibited the differentiation of osteoblastic MC3T3-E1 cells with FGF-2 contents ranging from 0.15 ± 0.03 to $0.31 \pm 0.04\ \mu g\ cm^{-2}$ [22]. Research on the FGF-2–AsMg–Ap layer on endothelial cell proliferation and function was very limited. Herein, the effect of the FGF-2–AsMg–Ap layer on endothelial cell proliferation and function was studied. FGF-2 is a wide-spectrum mitogenic, angiogenic and neurotrophic

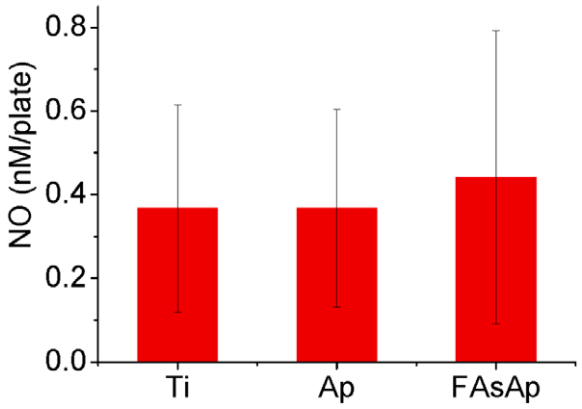

Figure 8. Nitric oxide (NO) release from HUVECs on as-prepared Ti, Ap and FAsAp coated Ti plates after 3 days of culture.

factor for a variety of cell types [14]. FGF-2 is an important regulator of endothelial cell proliferation, migration and protease production [13, 32, 33]. For example, surface bound FGF-2 accelerates endothelial cell proliferation [34, 35]. Ascorbic acid has been supplemented for culture of various cell types including endothelial cells [36, 37]. L-ascorbic acid 2-phosphate accelerated proliferation and extended the replicative lifespan of human corneal endothelial cells [38]. L-ascorbic acid 2-phosphate and FGF-2 showed a synergetic effect promoting the proliferation of human corneal endothelial cells than only L-ascorbic acid 2-phosphate or FGF-2 [38]. Similarly, the FGF-2–AsMg–Ap layer showed the highest HUVEC proliferation compared to Ap, FAp and AsAp coated Ti plates after 3 days of culture (figure 7).

HUVECs on FAsAp coated Ti showed a slightly higher, but not statistically significant, NO content than apatite coated and as-prepared Ti (figure 8). The synthesis of NO is an important marker of endothelial cell functionality and health, which is crucial in the control of smooth muscle cell proliferation, and platelet adhesion to the endothelial surface [16]. NO has been demonstrated to be a potent anti-platelet agent that can prevent thrombosis formation [39, 40]. NO deficiency also enhances smooth muscle cell proliferation and platelet aggregation and adhesion [41]. FGF-2 induces NO release from a number of cell types, including endothelial cells [42]. FGF-2 treatment of endothelial cells leads to increased production of biologically active NO [42]. Ascorbic acid prevents endothelial dysfunction by increasing release of NO from endothelial cells [15, 36].

The tissue-engineered endothelium layer markedly inhibited *in vitro* platelet adhesion (figures 9 and 10). Platelet adhesion is a critical index for evaluating the thrombogenic property of a blood-contacting implant. When an implant surface is exposed to blood, plasma proteins are adsorbed to the surface, followed by platelet adhesion. Activated platelets can recruit more platelets to aggregate on the surface that leads to thrombus formation [43]. The present results of platelet adhesion and NO content indicated that HUVEC growth and function are maintained normally on FGF-2–AsMg–Ap coated Ti surfaces. Further *in vivo* study is required.

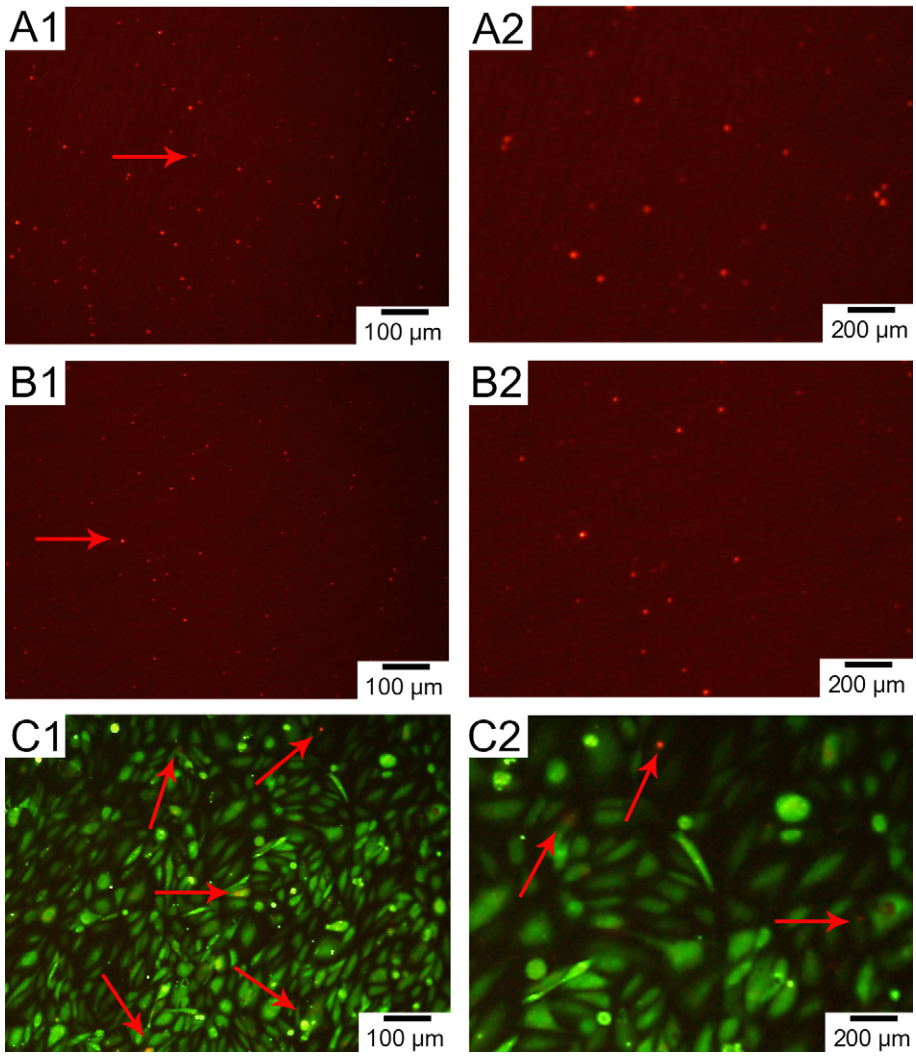

Figure 9. Fluorescence microscopy images of platelets adhered to Ti (A1, A2), Ap (B1, B2) and FAsAp + HUVEC coated Ti (C1, C2). HUVECs were stained for green fluorescence. Platelets were stained for red fluorescence (red arrows).

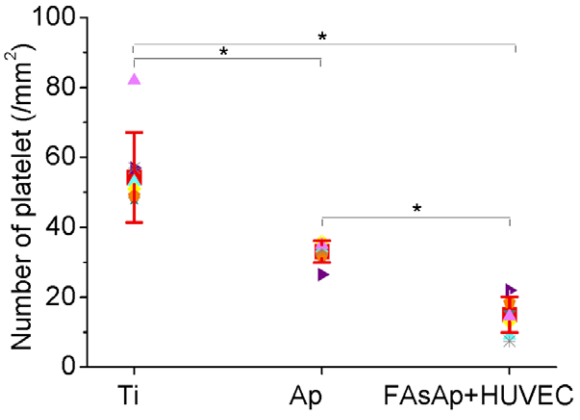

Figure 10. Number of platelets adhered to Ti, Ap and FAsAp+HUVEC coated Ti.

5. Conclusions

A tissue-engineered antithrombotic layer was prepared on titanium by coprecipitation of FGF-2, AsMg and apatite followed by endothelial cell seeding and culturing *in vitro*. The FGF-2–AsMg–Ap coated Ti plate was prepared by immersing the Ti plate in supersaturated calcium phosphate solutions supplemented with FGF-2 and AsMg. The FGF-2–AsMg–Ap layer on the Ti plate accelerated HUVEC proliferation. The tissue-engineered endothelial layer showed slightly higher nitric oxide release from HUVECs than apatite coated and as-prepared Ti, which indicated that the endothelial layer maintained proper function of the endothelial cells. The endothelial layer markedly inhibited *in vitro* platelet adhesion. Therefore, the tissue-engineered endothelial layer formed on the FGF-2–AsMg–Ap layer is promising for ameliorating platelet activation and thrombus formation on cardiovascular implants.

Acknowledgment

Fupo He was a China Scholarship Council (CSC) scholarship recipient (2011615041).

References

[1] Lietz K and Miller L W 2008 *Semin. Thorac. Cardiovasc. Surg.* **20** 225
[2] Schillinger M, Sabeti S, Dick P, Amighi J, Mlekusch W, Schlager O, Loewe C, Cejna M, Lammer J and Minar E 2007 *Circulation* **115** 2745
[3] Pagani F D *et al* 2009 *J. Am. Coll. Cardiol.* **54** 312
[4] Toyoda K 2009 *Drugs* **69** 633
[5] Baigent C, Sudlow C, Collins R, Peto R and Collaborat A T 2002 *Br. Med. J.* **324** 71
[6] van der Hoeven B L, Pires N M, Warda H M, Oemrawsingh P V, van Vlijmen B J, Quax P H, Schalij M J, van der Wall E E and Jukema J W 2005 *Int. J. Cardiol.* **99** 9
[7] Maisel W H 2007 *N. Engl. J. Med.* **356** 981
[8] Chen J L, Chen C, Chen Z Y, Li Q L and Huang N 2010 *J. Biomed. Mater. Res.* A **95** 341
[9] Cines D B *et al* 1998 *Blood* **91** 3527
[10] Garg U C and Hassid A 1989 *J. Clin. Invest.* **83** 1774
[11] Vane J R and Botting R M 1995 *Am. J. Cardiol.* **75** 3A
[12] Lee J G and Kay E D P 2006 *Invest. Ophthalmol. Vis. Sci.* **47** 1376
[13] Sahni A and Francis C W 2004 *Blood* **104** 3635
[14] Seghezzi G, Patel S, Ren C J, Gualandris A, Pintucci G, Robbins E S, Shapiro R L, Galloway A C, Rifkin D B and Mignatti P 1998 *J. Cell Biol.* **141** 1659
[15] Ladurner A, Schmitt C A, Schachner D, Atanasov A G, Werner E R, Dirsch V M and Heiss E H 2012 *Free Radic. Biol. Med.* **52** 2082
[16] Huang A, Vita J A, Venema R C and Keaney J F 2000 *J. Biol. Chem.* **275** 17399
[17] Sellers R S, Zhang R, Glasson S S, Kim H D, Peluso D, D'Augusta D A, Beckwith K and Morris E A 2000 *J. Bone Jt Surg. Am.* **82** 151
[18] Bonadio J 2000 *Adv. Drug Deliv. Rev.* **44** 185
[19] Nur-E-Kamal A, Ahmed I, Kamal J, Babu A N, Schindler M and Meiners S 2008 *Mol. Cell. Biochem.* **309** 157
[20] Wang X P, Li X, Onuma K, Ito A, Sogo Y, Kosuge K and Oyane A 2010 *J. Mater. Chem.* **20** 6437
[21] Li X, Wang X P, Ito A, Sogo Y, Cheng K and Oyane A 2009 *Mater. Sci. Eng.* C **29** 216
[22] Wang X P, Ito A, Sogo Y, Li X, Tsurushima H and Oyane A 2009 *Acta Biomater.* **5** 2647
[23] Wang X P, Ito A, Sogo Y, Li X and Oyane A 2010 *Acta Biomater.* **6** 962
[24] Wang X P, Ito A, Sogo Y, Li X and Oyane A 2010 *J. Biomed. Mater. Res.* A **92A** 1181
[25] Wang X, Ito A, Li X, Sogo Y and Oyane A 2011 *Biofabrication* **3** 022001
[26] Wang X P, Oyane A, Tsurushima H, Sogo Y, Li X and Ito A 2011 *Biomed. Mater.* **6** 045004
[27] Oyane A, Wang X P, Sogo Y, Ito A and Tsurushima H 2012 *Acta Biomater.* **8** 2034
[28] Muramatsu K, Uchida M, Kim H M, Fujisawa A and Kokubo T 2003 *J. Biomed. Mater. Res.* A **65** 409
[29] Li X, Wang X, Sogo Y, Ohno T, Onuma K and Ito A 2013 *Adv. Healthc. Mater.* 10.1002/adhm.201200149
[30] Wang X, Li X, Ito A, Sogo Y and Ohno T 2013 *Acta Biomaterialia* 10.1016/j.actbio.2013.03.031
[31] Wang X P, Ito A, Li X, Sogo Y, Hirose M, Oyane A and Tsurushima H 2013 *Mater. Sci. Eng.* C **33** 512
[32] Gospodarowicz D, Ferrara N, Schweigerer L and Neufeld G 1987 *Endocr. Rev.* **8** 95
[33] Edelman E R, Nugent M A, Smith L T and Karnovsky M J 1992 *J. Clin. Invest.* **89** 465
[34] Underwood P A, Whitelock J M, Bean P A and Steele J G 2002 *J. Biomater. Sci. Polym. Ed.* **13** 845
[35] Nicaeus T E, Tolentino M J, Adamis A P and Rubin P A D 1996 *Ophthal. Plast. Reconstr. Surg.* **12** 235
[36] May J M 2000 *Free Radic. Biol. Med.* **28** 1421
[37] Engelmann K and Friedl P 1995 *Cornea* **14** 62
[38] Shima N, Kimoto M, Yamaguchi M and Yamagami S 2011 *Invest. Ophthalmol. Vis. Sci.* **52** 8711
[39] Major T C, Brant D O, Reynolds M M, Bartlett R H, Meyerhoff M E, Handa H and Annich G M 2010 *Biomaterials* **31** 2736
[40] Riccio D A, Dobmeier K P, Hetrick E M, Privett B J, Paul H S and Schoenfisch M H 2009 *Biomaterials* **30** 4494
[41] Shaul P W 2002 *Annu. Rev. Physiol.* **64** 749
[42] Kostyk S K, Kourembanas S, Wheeler E L, Medeiros D, McQuillan L P, D'Amore P A and Braunhut S J 1995 *Am. J. Physiol.* **269** H1583
[43] Sivaraman B and Latour R A 2010 *Biomaterials* **31** 832